JACS
JOURNAL OF THE AMERICAN CHEMICAL SOCIETY
Article
pubs.acs.org/JACS

Unique Transformation from Graphene to Carbide on Re(0001) Induced by Strong Carbon−Metal Interaction

Yue Qi,[†] Caixia Meng,[‡] Xiaozhi Xu,[§] Bing Deng,[†] Nannan Han,[∥] Mengxi Liu,[⊥] Min Hong,[#] Yanxiao Ning,[‡] Kaihui Liu,[§] Jijun Zhao,[∥] Qiang Fu,[‡] Yuanchang Li,*[,∇] Yanfeng Zhang,*[,†,#,○] and Zhongfan Liu*[,†,○]

[†]Center for Nanochemistry (CNC), Academy for Advanced Interdisciplinary Studies, Beijing National Laboratory for Molecular Sciences, College of Chemistry and Molecular Engineering, Peking University, Beijing 100871, People's Republic of China

[‡]State Key Laboratory of Catalysis, Dalian Institute of Chemical Physics, The Chinese Academy of Sciences, Dalian 116023, People's Republic of China

[§]State Key Laboratory for Mesoscopic Physics, School of Physics, Academy for Advanced Interdisciplinary Studies, Peking University, Beijing 100871, People's Republic of China

[∥]Key Laboratory of Materials Modification by Laser, Ion and Electron Beams, Dalian University of Technology, Ministry of Education, Dalian 116024, People' s Republic of China

[⊥]CAS Key Laboratory of Standardization and Measurement for Nanotechnology, CAS Center for Excellence in Nanoscience, National Center for Nanoscience and Technology, Beijing 100190, People's Republic of China

[#]Department of Materials Science and Engineering, College of Engineering, Peking University, Beijing 100871, People's Republic of China

[∇]Advanced Research Institute of Multidisciplinary Science, Beijing Institute of Technology, Beijing 100081, People's Republic of China

[○]Beijing Graphene Institute (BGI), Beijing 100095, People's Republic of China

Supporting Information

ABSTRACT: During graphene growth on various transition metals in the periodic table, metal carbides always emerge to behave as complex intermediates. On VIII metals, metastable carbides usually evolve and then transform into graphene along the phase interfaces, and even no metal carbides can form on IB−IIB metals. In contrast, during graphene growth on group IVB−VIB metals, carbides are usually generated even before the evolution of graphene and stably exist throughout the whole growth process. However, for the remaining transition metals, e.g., group VIIB, located in between IVB−VIB and VIII, the interplay between graphene and carbide is still vague. Herein, on Re(0001) (VIIB), we have revealed a novel transition from graphene to metal carbide (reverse to that on VIII metals) for the first time. This transition experienced graphene decomposition, dissolution, and carbon segregation processes, as evidenced by scanning tunneling microscopy (STM) and on-site, variable-temperature low electron energy diffraction (LEED) characterizations. This work thus completes the picture about the interplay between graphene and carbide on/in transition metals in the periodic table, as well as discloses a new territory for the growth of carbon-related materials, especially the metal carbide.

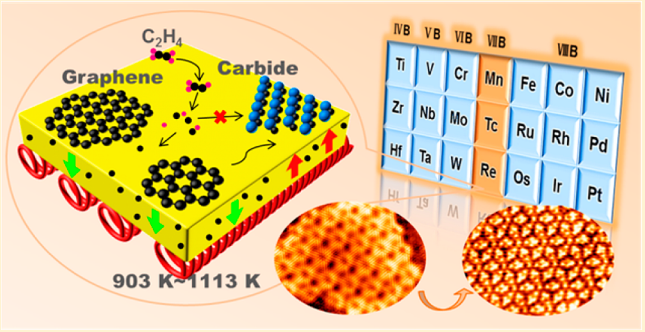

INTRODUCTION

The synthesis of carbon-related materials, such as graphene and metal carbides, is usually realized via the chemical vapor deposition (CVD) process on transition metals through the dehydration of hydrocarbons.[1−7] For instance, on group VIB metal of Mo, large-area, high-quality two-dimensional (2D) ultrathin Mo_2C crystals have been synthesized through a facile CVD method, which presents intriguing thickness-dependent superconductivity.[1] However, the preferential chemical states of carbon in the relevant products (e.g., graphene or carbide) correlate strongly with the periodic physicochemical properties of metal elements in the periodic table (e.g., carbon solubility and carbon affinity), as well as reaction conditions (e.g., annealing temperature and carbon dosage).[1,4,5,8−10] What's more, on various metal substrates, the growth processes of graphene and carbide present divergent interplays, including

Received: September 15, 2017
Published: November 14, 2017

DOI: 10.1021/jacs.7b09755
J. Am. Chem. Soc. 2017, 139, 17574−17581

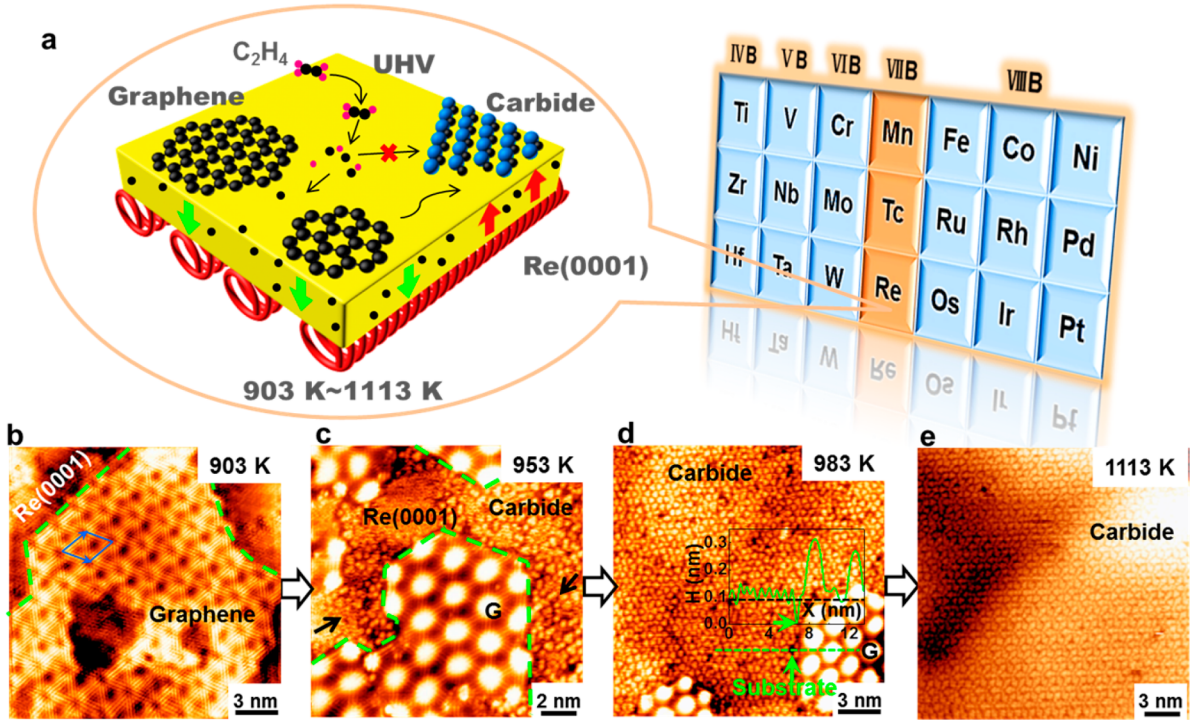

Figure 1. Transition from graphene to metal carbides by ascending the annealing temperature of as-deposited graphene on Re(0001). (a) Schematic of the UHV system for growing graphene and rhenium carbide on Re(0001), one of the group VIIB metals located in between groups IVB−VIB and VIII in the periodic table. (b) Graphene synthesized by exposing Re(0001) to C_2H_4 at ∼903 K for 20 min. (c) Annealing the sample in part b at ∼953 K for ∼30 min, leading to the reduction of graphene coverage and the generation of a novel disordered structure (black arrows). (d) Annealing the sample in part c at ∼983 K for another ∼30 min, leading to the evolution of more uniform structures with an increased coverage, accompanied by the shrinkage of graphene coverage. Inset: height profile riding over the two components (green arrows pointing to the bare substrate). (e) Periodic "flower-like" superstructure evolved after ∼1113 K annealing for another ∼30 min. Scanning conditions: (b) −0.01 V, 3.33 nA; (c) −0.01 V, 2.42 nA; (d) −0.02 V, 1.06 nA; (e) −0.02 V, 5.03 nA.

the evolution of the single phase, coexistence of the above two phases, and their transition.[2−4,8,11]

For group IB−IIB metals featured with relatively low carbon solubility and weak carbon−metal interaction (e.g., Cu[2,8] and Au[11]), corresponding carbides even cannot evolve under graphene formation conditions.[12] Therefore, no carbide participates in the growth of graphene, and a self-limited growth behavior usually results under a surface catalytic mechanism. With regard to group VIII metals, metastable carbides usually evolved at the initial growth stage, which was then transformed into graphene through a high-temperature annealing process.[4,5,13] For instance, on the representative Ni(111) substrate, metastable Ni_2C formed upon the hydrocarbon exposure (around ∼460 °C) could be transformed into graphene along the one-dimensional phase interface through the in-plane carbon migration, as evidenced by Auger spectra and STM characterizations.[4]

When moving to group IVB−VIB metals, however, their carbides present better stability than that of groups IB−IIB and VIII metals. Carbides were generated even before the formation of graphene, and stably existed throughout the whole growth process.[3] Actually, the carbide formation could be utilized to favor the precise layer control to preferentially achieve the monolayer graphene. This is because, on one hand, the appearance of carbide could weaken the carbon affinity of the catalyst's surface and reduces the possibility for carbon atoms to go through the evolved monolayer to form a second layer;[14] on the other hand, the extremely stable metal carbide formed by the in situ conversion of dissolved carbon could suppress the upward segregation/precipitation of carbon atoms,[3] therefore lowering the possibility for the second layer growth.

In general, for transition metals located at different groups in the periodic table, the mutual transition between graphene and carbide is obviously diverse, and most of them have been well clarified. However, for the remaining transition metals, i.e., group VIIB, located in between groups IVB−VIB and VIII, the related studies are still lacking, let alone the atomic-scale insight of the specific structures. This kind of research will fill the void in our understanding about graphene growth on transition metals. Herein, we chose Re(0001) as the representative substrate, on which a new phase of rhenium carbide was detected for the first time. Its detailed structure (ReC) was addressed by combining high-resolution STM, LEED, and density functional theory (DFT) investigations. More importantly, a novel transition from the first-formed graphene to rhenium carbide was captured under a stepwise high-temperature annealing procedure, in which graphene decomposition and dissolution and carbon segregation processes were visually investigated by on-site variable-temperature LEED observations. Notably, such a transition tendency/pathway on Re(0001) is in sharp contrast to that on the neighboring group VIII metals, as discussed above.[4,5,13,15]

■ RESULTS AND DISCUSSION

The schematic of the ultrahigh vacuum chemical vapor deposition (UHV-CVD) system for graphene and rhenium carbide growth is presented in Figure 1a (see growth details in Figure S1a). Re(0001), being a representative single crystal for

DOI: 10.1021/jacs.7b09755
J. Am. Chem. Soc. 2017, 139, 17574−17581

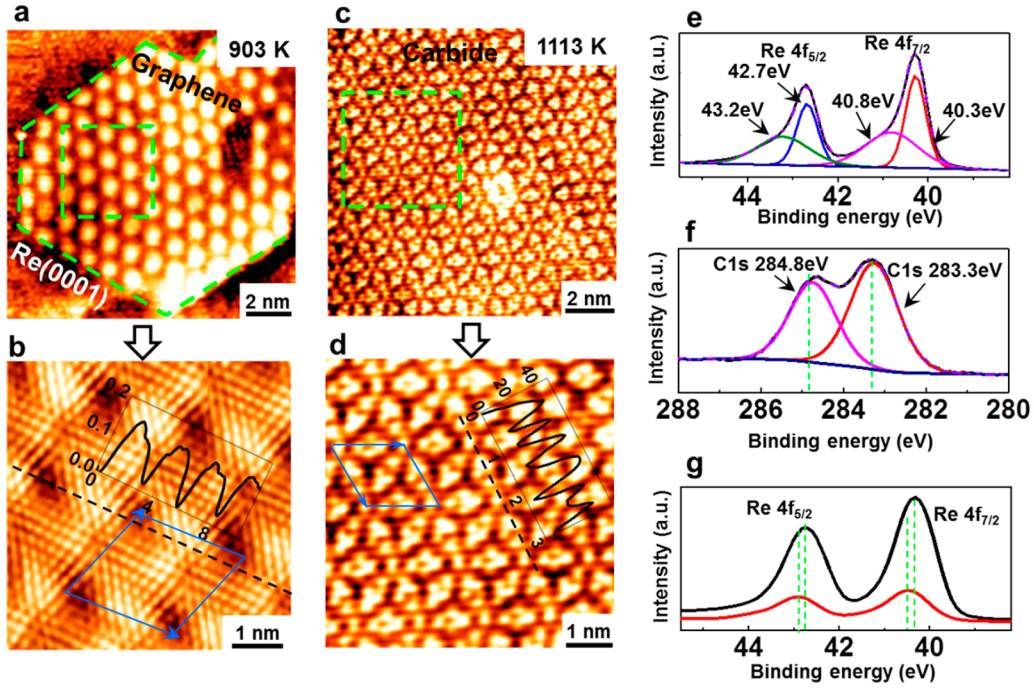

Figure 2. Morphology and compositional analyses of the individually synthesized graphene or rhenium carbide on Re(0001). (a, b) STM images of graphene featured with uniform moiré and atomic lattices with periods of ∼2.48 and ∼0.25 nm, respectively. Inset in part b: height profile along the line showing graphene surface corrugation of ∼0.16 nm. (c) STM image of the six-petal "flower-like" structure on Re(0001), showing a hexagonally symmetric superstructure with a period of ∼1.44 nm. (d) High-resolution STM image from the marked area in part c presenting atomic-scale contrasts in each petal. Inset: height profile along the line showing the atomic period of ∼0.39 nm and surface corrugation of ∼0.03 nm, respectively. (e, f) XPS spectra of Re 4f and C 1s from the "flower"-covered Re(0001). (g) Re 4f spectra from the "flower"-covered Re(0001), measured under the normal (black line) and grazing modes (inclined by an angle of ∼70°) (red line). Scanning conditions: (a) −0.06 V, 8.10 nA; (b) −0.01 V, 11.49 nA; (c, d) −0.01 V, 2.35 nA.

the group VIIB metals, is chosen as the growth substrate in this work. When Re(0001) was exposed to C_2H_4 for ∼20 min at ∼903 K (vacuum changing from $\sim 1.0 \times 10^{-10}$ to $\sim 5.0 \times 10^{-9}$ mbar) (process (1) in Figure S1a), monolayer graphene emerged on the substrate surface, as characterized with the formation of the uniform moiré superstructure with a fixed period of ∼2.48 nm,[16,17] originating from the lattice mismatch between graphene and Re(0001) (STM image in Figure 1b captured at room temperature). However, after sample annealing at ∼953 K for ∼30 min, the coverage of graphene began to reduce, accompanied by the evolution of some disordered "special structures", randomly distributing on the bare substrate (as marked by black arrows in the STM image in Figure 1c). Subsequently, after further sample annealing at ∼983 K for ∼30 min, the "special structures" became more ordered and the coverage was increased accordingly. Concurrently, the coverage of graphene was dramatically decreased, leaving only smaller domains on the surface (Figure 1d). Notably, the inset height profile riding over the two components revealed that the two types of structures were almost located on the same atomic plane, irrespective of their large surface corrugation difference (∼0.16 nm vs ∼0.03 nm for graphene and carbide, respectively). And the arrows both in the curve and in the STM image marked the locations down to the bare substrate. Furthermore, after sample annealing at ∼1113 K for ∼30 min, only uniform "flower-like" patterns appeared on the substrate surface (Figure 1e). Briefly, the whole transformation process from graphene to the special "flower-like" structure is simply displayed in the schematic in Figure 1a, and the detailed transformation mechanism will be illustrated in the latter part of the work.

As mentioned above, when Re(0001) was kept at ∼903 K under the C_2H_4 atmosphere, hexagonal graphene domains usually formed on the substrate surface (Figure 2a). And the atomically resolved STM image exhibits perfect graphene moirés and atomic lattices with fixed periods of ∼2.48 and ∼0.25 nm, respectively (Figure 2b). The moiré superstructure actually arises from a coincidence lattice of (10 × 10) C−C/(9 × 9) Re(0001), which agrees well with the reported results for graphene on Re(0001).[16−18] This coincidence can be calculated from the following equation

$$D = \frac{(1+\delta)a}{\sqrt{2(1+\delta)(1-\cos\theta)+\delta^2}}$$

where D, θ, a, and δ denote the graphene moiré period, the rotation angle between the graphene and Re(0001) lattices, the lattice constant of graphene (∼0.246 nm), and the lattice mismatch (∼11.4%) between graphene and Re(0001), respectively. The calculated rotation angle between graphene and Re(0001) was 0°, highly indicative of an epitaxial growth behavior. The surface corrugation for graphene is ∼0.16 nm (inset in Figure 2b), consistent with the calculated value of ∼0.13 nm.[19] Particularly, this value is even larger than that on Rh(111) (∼0.118 nm, calculated with the same DFT method),[20] a commonly known strongly interacting metal substrate. In addition, for graphene on Re(0001), the calculated binding energy (BE) per Re atom was ∼0.54 eV,[19] which is much higher than that for graphene on Rh(111) (∼0.36 eV)[20] and Ir(111)[21] (∼0.32 eV). All of these clues imply the extremely strong interface interaction between graphene and Re(0001) substrate.

DOI: 10.1021/jacs.7b09755
J. Am. Chem. Soc. 2017, 139, 17574−17581

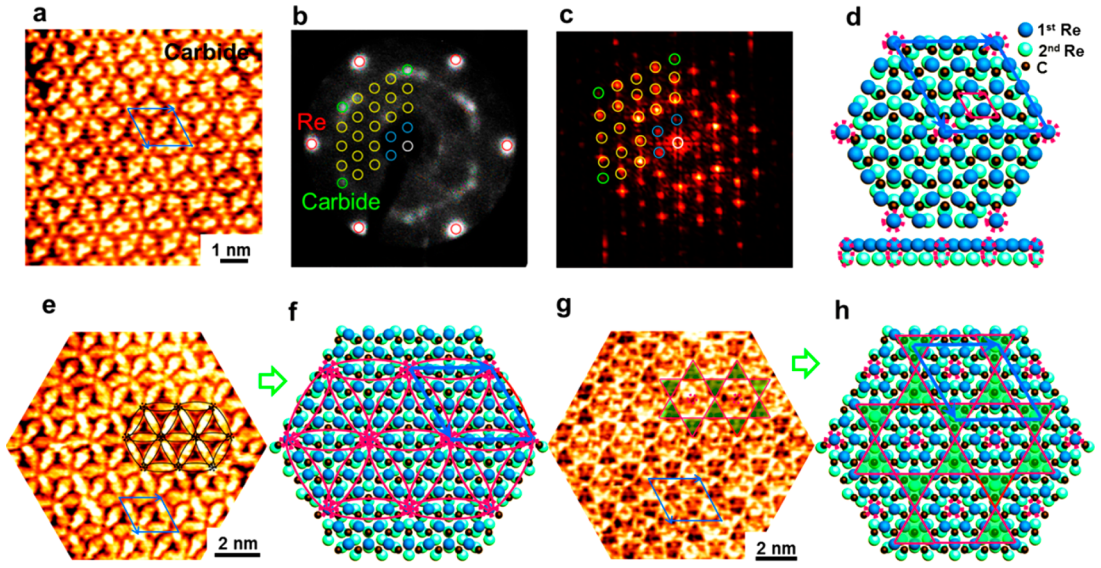

Figure 3. Structural identification and theoretical simulation of the "flower-like" rhenium carbide on Re(0001). (a) STM image of rhenium carbide. (b) LEED pattern showing hexagonal diffraction spots of carbide (green circles), with a rotation angle of 30° relative to the Re(0001) substrate (red circles) and a lattice constant of ∼0.36 nm. (c) FFT of the STM image in part a. Spots marked by green and blue circles arise from the atom and superstructure of the carbide, respectively. (d) DFT calculated structure of rhenium carbide with only one Re and C atoms in a rhombic unit cell (marked by red lines). (e, g) Varying STM patterns of the carbide superstructure under different scanning conditions. (f, h) Simulated patterns of carbide on Re(0001) based on the different spatial occupations, well consistent with the STM patterns in parts e and g, respectively. Scanning conditions: (a) −0.01 V, 2.35 nA; (e) −0.11 V, 0.93 nA; (g) −0.01 V, 20.36 nA.

Notably, the special "flower-like" structure appearing in Figure 1e could also be achieved through directly exposing Re(0001) to C_2H_4 at ∼1113 K (process (2) in Figure S1a). Full-layer "flower-like" structures with a period of ∼1.44 nm were observed after the sample cooling down to RT (Figure 2c). In the high-resolution STM image (Figure 2d), atomic-scale contrast variations with a period of ∼0.39 nm could also be distinguishable in every petal of the "flower-like" superstructure (inset curve), possibly due to the arrangements of the surface atoms.

Considering that only C_2H_4 precursor was used in the growth process under the base vacuum better than 1×10^{-10} mbar, along with the fact that the lattice constant and superstructure period are much different from that of graphene, rhenium carbide is thus proposed to be evolved on the substrate surface. To confirm this, XPS characterization of the "flower"-covered sample was then carried out. According to the reported work, the strong C−Re bonds in rhenium carbide could induce new Re $4f_{7/2}$ and $4f_{5/2}$ peaks at higher binding energies (BEs), with regard to the Re bulk component (∼570 meV higher).[22] In this work, for the "flower"-covered Re(0001), the deconvolutions of Re $4f_{7/2}$ and $4f_{5/2}$ spectra both present one new component at higher BEs (∼40.8 and ∼43.2 eV, respectively, Figure 2e), which are distinguished from the pristine components of the clean substrate (Re $4f_{7/2}$, ∼40.3 eV; $4f_{5/2}$, ∼42.7 eV, Figure S2b). This data is thus considered as the tentative proof for the formation of rhenium carbide. Additionally, according to the published reference, the charge transfer between metal and carbon could partly represent the strength of the carbon−metal interaction.[23] Specifically, the higher BE components in Re $4f_{7/2}$ and $4f_{5/2}$ peaks imply obvious negative charge donation from Re to C atoms, thus addressing the relatively strong C−Re interaction.[24] Moreover, in the C 1s curve, a new component at a lower BE of ∼283.3 eV also appeared (Figure 2f, measured under grazing mode with an inclined angle of ∼70°), which is consistent with the reported C 1s peak of rhenium carbide at ∼283.35 eV.[22] And the C 1s peak centered at ∼284.8 eV is always considered as the pollution carbon.

To evaluate the vertical distribution of rhenium carbide on/in Re(0001), XPS measurements under the normal and grazing modes were both carried out for comparison (black and red lines in Figure 2g, respectively). Under the grazing mode with an inclined angle of ∼70° (red line), the intensity of Re $4f_{7/2}$ and $4f_{5/2}$ peaks is obviously reduced; however, the shoulders of these peaks at high BEs become more obvious, compared with that measured under the normal mode (black line). Moreover, the Re $4f_{7/2}$ and $4f_{5/2}$ peaks of the inclined sample shift to higher BEs with regard to the normal one. These obvious differences further indicate that the rhenium carbide is located on the substrate surface, well consistent with the morphology and the height profile analyses of carbide and graphene on the Re(0001) surface in Figure 1d.

The rhenium carbide on Re(0001) was also characterized by LEED to obtain the lattice constant and the relative rotation between carbide and substrate. As shown in Figure 3b, hexagonal diffraction spots (green circles) show a rotation angle of 30° relative to the Re(0001) substrate (red circles), presenting a lattice constant of ∼0.36 nm, which is very close to the distance between adjacent atomic-scale contrasts distinguished in Figure 2d (∼0.39 nm). Hence, this group of diffraction spots possibly arises from C and Re atoms in the surface rhenium carbide. Moreover, a group of (4 × 4) spots with a period of ∼1.44 nm was also observed (blue circles), corresponding to the "flower-like" superstructure in the STM image in Figure 3a. The detailed ascriptions of the LEED patterns are supplemented in Figure S3a. Moreover, Figure 3c displays the FFT spots from the STM image in Figure 3a. The green- and blue-marked spots possess periods of ∼0.36 and ∼1.44 nm, respectively, corresponding to the periods of the atom and superstructure of rhenium carbide on Re(0001), respectively (Figure 2d).

DOI: 10.1021/jacs.7b09755
J. Am. Chem. Soc. 2017, 139, 17574−17581

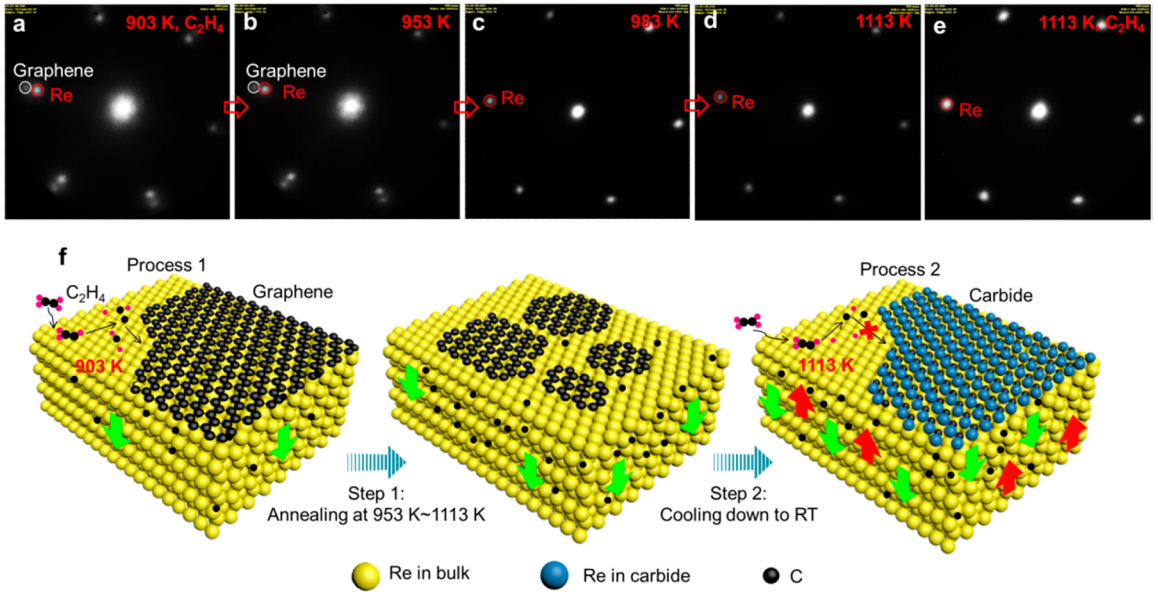

Figure 4. On-site, variable-temperature LEED characterizations revealing the transition from graphene to rhenium carbide on Re(0001). (a) LEED pattern for graphene synthesized at ~903 K under the C_2H_4 atmosphere (the patterns for graphene and Re(0001) marked with white and red circles, respectively). (b–d) LEED for the sample in part a upon stepwise annealing at ~953 K (b), ~983 K (c), and ~1113 K (d) for ~30 min, respectively. At ~983 K, graphene disappeared, as evidenced by the missing of the characteristic LEED pattern. (e) LEED for the sample obtained at ~1113 K under the C_2H_4 atmosphere. Neither graphene nor carbide appeared. (f) Schematics for the growth of graphene and carbide, and their transformation mechanism on Re(0001).

Notably, identical LEED patterns and STM images were also observed on the entire sample (5 mm × 5 mm), highly indicative of the formation of the large-area, homogeneous carbide film on Re(0001). The XPS and LEED characterizations are actually carried out in different apparatus. That means, the samples have to be exposed to the atmosphere before loading into other systems for subsequent characterizations. This compatibility with different analytical techniques again confirms that the rhenium carbide presents good stability even under the atmospheric conditions.

As discussed above, the STM, LEED, and FFT characterizations provide the consistent structure information on rhenium carbide on Re(0001). However, various possible structures satisfying the above analyses can be figured out, including ReC_2, C_4, Re_2C, and ReC (Figure S4). However, after DFT relaxation, all of the structures become irregular on Re(0001), except for ReC (Figure 3d). It was thus regarded as the most possible structure of the observed rhenium carbide. In the rhombic unit cell of this model, only one Re atom and one C atom are contained, which is consistent with the appearance of a single new component in C 1s (~283.3 eV), Re $4f_{7/2}$ (~40.8 eV), and Re $4f_{5/2}$ (~43.2 eV) (Figure 2). In addition, the monatomic layer feature of ReC is also convinced by the height analysis of rhenium carbide on Re(0001) by STM, with graphene as a reference (Figure 1d). To our knowledge, this rhenium carbide phase has never been reported before, and thus should enrich our knowledge about the family of metal carbides.

STM imaging of the moiré superstructure always displays a strong electronic effect, leading to varying patterns under different scanning conditions. Specifically, the STM contrasts vary with the relative locations of carbon atoms with the underlying metal atoms, as well as the density of electronic states at the specific scanning energy, as illustrated in detail for graphene/Ru(0001).[25] The varying patterns of the superstructures for ReC/Re(0001) were also captured under different scanning conditions ((e) −0.11 V, 0.93 nA; (g) −0.01 V, 20.36 nA) (Figure 3e and g). Notably, the corresponding simulated patterns in Figure 3f and h (red lines), extracted from the different spatial occupations of ReC on Re(0001), present a good coincidence with the STM images. Such a consistence gives complementary proof of the proposed structure of rhenium carbide.

The underlying growth mechanism of graphene and carbide and their interplay on Re(0001) should be an intriguing issue. In the reported work about the carbon interaction with the rhenium surface,[26] at $T > 750$ K, the thermal decomposition of C_2H_4 on Re(0001) could result in three processes: graphene growth, dissolution of C atoms into bulk Re, and surface carbide formation. This makes the growth mechanisms of graphene and carbide quite complicated under a similar growth process. However, due to the high carbon solubility of Re bulk around such a high temperature (e.g., ~4.39% (at) at ~1000 °C),[27] the carbon dissolution into Re bulk always prevails over the surface reactions. This was supported by a previous result that, when a C atom beam was directed onto a carbon-free Re substrate at ~865 K, although the carbon dosage is sufficient for the formation of five-layer-thick carbon layers, the Re surface was free of C atoms, and all of them dissolved into the Re bulk.[26]

As illustrated in the STM image in Figure 2a, when C_2H_4 was introduced into the UHV-CVD system with substrate held at ~903 K, only graphene formed on the surface, as convinced by the on-site, high-temperature LEED characterization in Figure 4a. In this process, a large amount of carbon atoms concurrently dissolved into the Re bulk. Specifically, when the carbon injection rate is higher than the dissolution rate, carbon pieces have a higher possibility to be maintained on the substrate surface and transform into graphene, as displayed in process 1 in Figure 4f. Moreover, under such low growth

DOI: 10.1021/jacs.7b09755
J. Am. Chem. Soc. 2017, 139, 17574–17581

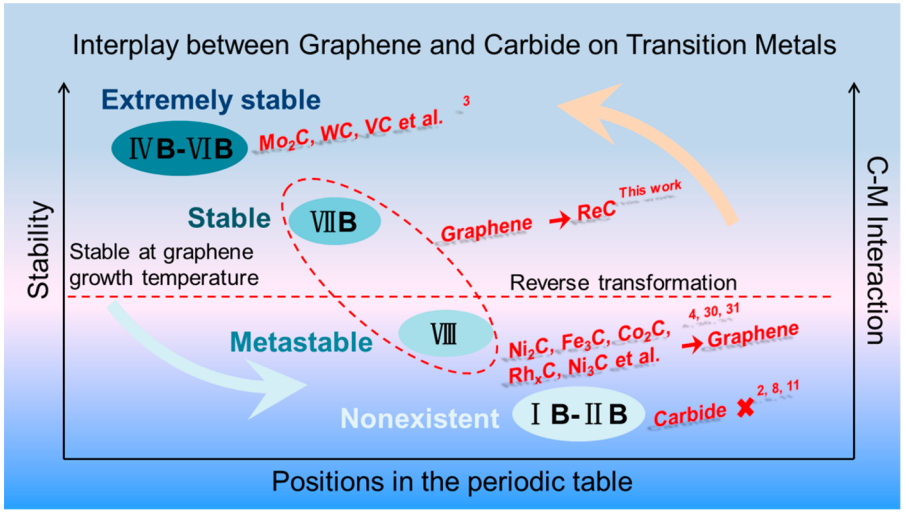

Figure 5. Summary of the interplay between graphene and carbide on the transition metals in the periodic table during graphene growth, presenting the increased carbon−metal interaction and the stability of the metal carbides from right to left, respectively.

temperature, no carbide evolved on the Re surface, which was totally distinct from that on group IVB−VIB metals, where carbides appeared even before graphene, and stably existed throughout the whole growth process.[3,28]

Upon being exposed to C_2H_4 at ∼1113 K, the substrate was fully covered with rhenium carbide, as observed from the STM image after sample cooling down to RT (Figure 2c). However, according to the reported result,[26] a relatively high temperature up to 1500 K is the prerequisite for the externally introduced C atoms to react with the surface Re atoms to form carbide, along with the rearrangement of Re atoms. Accordingly, in this work, the possibility for carbide formation through the direct surface reaction route is low at a relatively low temperature of ∼1113 K. Actually, the on-site, high-temperature (∼1113 K) LEED characterization in Figure 4e confirmed that no carbide formed on the surface in this growth state. However, after sample cooling down to RT, rhenium carbide appeared on the surface, as displayed in Figure 3a and b.

Interestingly, when no external carbon precursors (C_2H_4) were introduced into the UHV system, i.e., only after substrate annealing at ∼1113 K and cooling down to RT, the Re surface was still covered with an ordered carbide phase (process (4) in Figure S1a and STM images in Figure S5a and b). During this process, the UHV chamber was kept at a good vacuum of better than 1×10^{-10} mbar, and the only possible carbon source to form carbide was the C atoms dissolved into the Re bulk beforehand. In this regard, the pathway for rhenium carbide formation is through the carbon segregation process, as displayed in process 2 in Figure 4f. Intriguingly, such a segregated growth mechanism of rhenium carbide is a newly discovered characteristic of Re(0001), which provides a new pathway for carbide synthesis, as distinct from the commonly reported surface reaction route.[4,5] Specifically, the segregation growth route requires a lower temperature (∼1113 K) than that needed through the carbon surface reaction route (1500 K).[26]

It is evident that the segregated product on Re(0001) (rhenium carbide) is different from that on Rh[29] or Ni[9] (graphene). The failure for the segregation growth of graphene on Re(0001) could be explained from the extremely strong C−Re interaction. When C atoms dissolved into the Re bulk, the strong C−Re interaction could block their diffusion and preclude them from totally penetrating through the bulk to be free on the surface for graphene formation.

Furthermore, the on-site, variable-temperature LEED characterizations also provide the good restoration to the transition process displayed in the STM images in Figure 1. On the VIIB metal of Re(0001), the reverse transformation (from graphene to carbide) with regard to that on the neighboring VIII metals (from carbide to graphene) occurred through different transition pathways.[4,5,13] For instance, the conversion from Ni_2C to graphene on Ni(111) (group VIII) was along the 1D Ni_2C−graphene interface by the in-plane migration of surface carbon atoms from carbide to graphene.[4] However, on Re(0001), the carbide formation was not limited at the edges of graphene domains but distributed randomly on the bare substrate surface, as evidenced by the STM image in Figure 1c. This preliminarily excluded the mechanism of in-plane carbon migration at the phase interfaces. Moreover, the on-site, variable-temperature LEED characterizations directly present that graphene still existed under ∼953 K annealing for ∼30 min (Figure 4b) but disappeared at ∼983 K (Figure 4c). Upon higher-temperature annealing at ∼1113, ∼1123, ∼1173, and ∼1223 K, neither graphene nor carbide appeared on the Re(0001) surface (Figure 4d and Figure S6). However, after sample cooling down to RT, the rhenium carbide fully extended over the substrate surface, as presented in Figure 3a and b. In this regard, the transition from graphene to carbide on Re(0001) experienced complicated processes, i.e., the decomposition and dissolution of graphene upon high-temperature annealing, followed by carbon segregation during the cooling down process, as displayed in steps 1 and 2 in Figure 4f.

It is instructive to compare the interplay between graphene and carbide (e.g., their coexistence and transition) on Re(0001) with that on the other transition metals in the periodic table. For group IB−IIB metals featured with relatively low carbon solubility and weak carbon−metal interaction (e.g., Cu[2,8] and Au[11]), corresponding carbides cannot even form under graphene formation conditions. With regard to group VIII metals, Rh(111) was selected as an example, instead of Ni(111) as discussed above. First, graphene/Rh(111) could be stable over a considerably larger temperature range (808−1053 K)[15] than that of graphene/Re(0001) (903−953 K). Second, carbide on Rh(111) is energetically less stable than that of graphene,

DOI: 10.1021/jacs.7b09755
J. Am. Chem. Soc. 2017, 139, 17574−17581

which favors its transformation to graphene. Similar performance also happens to other group VIII metal carbides, such as Fe_3C[30] and Co_2C.[3,31]

In contrast, on the representative member of group VIIB metals, like Re(0001), rhenium carbide could be stable at the graphene formation temperature or even higher. In this work, after ab initio molecular dynamics (AIMD) simulation for 10 ps at 1050 K, the structure of ReC on Re(0001) was still maintained (Figure S7), implying its relatively high stability. And the reported desorption temperature of C atoms from rhenium carbide is up to ~2600 K,[26] as mediated by the extremely high carbon−metal bond strength. When moving to group IVB−VIB metals,[3] extremely strong carbon−metal interaction exists, and their carbides are formed even before the formation of graphene and stably exist throughout the whole graphene growth process. In this regard, the interplay between graphene and metal carbides can be tentatively summarized; i.e., the carbon−metal interaction increases from right to left for the transition metals in the periodic table, and the stability of metal carbides is steadily increased accordingly, as presented in Figure 5.

In summary, on the group VIIB metal of Re(0001), we have revealed a novel transition from graphene to metal carbide in the CVD growth process for the first time, which undergoes graphene decomposition, dissolution, and carbon segregation procedures. The transformation tendency/pathway is in sharp contrast to that on the neighboring group VIII metals. This work hereby completes the picture about the interplay between graphene and carbide in the CVD growth process on/in different groups of transition metals in the periodic table, and discloses a new territory for the synthesis of carbon-related materials, especially the metal carbide, which has presented wide applications in supercapacitors and lithium-ion batteries.[32−35]

METHODS

Sample Preparations. The Re(0001) substrate was pretreated via Ar^+ sputtering and annealing in the O_2 atmosphere, and postannealing at ~873 K under UHV conditions to remove surface impurities. Graphene and rhenium carbide were synthesized on Re(0001) with ethylene (C_2H_4) as precursor by heating the substrate to a specific temperature.

Characterizations. An Omicron VT-STM system was used for the high-resolution characterization, with a base pressure better than 10^{-10} mbar. All STM images were obtained at room temperature. The sample was moved out of the vacuum chamber for XPS and LEED measurements in other equipment. An Elmitec LEED/LEEM/PEEM system was used for on-site, variable-temperature LEED characterizations with a base pressure better than 10^{-10} Torr.

DFT Calculations. Geometry optimizations were calculated using the Vienna ab initio simulation package (VASP) within the framework of DFT. The Perdew−Burke−Ernzerhof generalized gradient approximation and the projector-augmented wave potential with a cutoff energy of 400 eV were used to describe the exchange-correlation energy and the electron−ion interaction, respectively.

ASSOCIATED CONTENT

Supporting Information

The Supporting Information is available free of charge on the ACS Publications website at DOI: 10.1021/jacs.7b09755.

The detailed growth processes and DFT calculations (PDF)

AUTHOR INFORMATION

Corresponding Authors

*zfliu@pku.edu.cn
*yanfengzhang@pku.edu.cn
*liyc@nanoctr.cn

ORCID

Kaihui Liu: 0000-0002-8781-2495
Jijun Zhao: 0000-0002-3263-7159
Qiang Fu: 0000-0001-5316-6758
Yanfeng Zhang: 0000-0003-1319-3270
Zhongfan Liu: 0000-0003-0065-7988

Notes

The authors declare no competing financial interest.

ACKNOWLEDGMENTS

The work was supported by the National Key Research and Development Program of China (2016YFA0200103), the Beijing Municipal Science and Technology Commission (No. Z161100002116020), the Open Research Fund Program of the State Key Laboratory of Low-Dimensional Quantum Physics (No. KF201601), the National Natural Science Foundation of China (Nos. 51290272, 51472008, 51432002, 50121091, and 21201012), and the National Basic Research Program of China (Nos. 2013CB932603, 2014CB921002).

REFERENCES

(1) Xu, C.; Wang, L.; Liu, Z.; Chen, L.; Guo, J.; Kang, N.; Ma, X.-L.; Cheng, H.-M.; Ren, W. *Nat. Mater.* **2015**, *14*, 1135−1141.
(2) Li, X.; Cai, W.; An, J.; Kim, S.; Nah, J.; Yang, D.; Piner, R.; Velamakanni, A.; Jung, I.; Tutuc, E.; Banerjee, S. K.; Colombo, L.; Ruoff, R. S. *Science* **2009**, *324*, 1312−1314.
(3) Zou, Z.; Fu, L.; Song, X.; Zhang, Y.; Liu, Z. *Nano Lett.* **2014**, *14*, 3832−3839.
(4) Lahiri, J.; Miller, T.; Adamska, L.; Oleynik, I. I.; Batzill, M. *Nano Lett.* **2011**, *11*, 518−522.
(5) Jacobson, P.; Stöger, B.; Garhofer, A.; Parkinson, G. S.; Schmid, M.; Caudillo, R.; Mittendorfer, F.; Redinger, J.; Diebold, U. *ACS Nano* **2012**, *6*, 3564−3572.
(6) Cheon, J.; Dubois, L. H.; Girolami, G. S. *J. Am. Chem. Soc.* **1997**, *119*, 6814−6820.
(7) Girolami, G. S.; Jensen, J. A.; Pollina, D. M.; Allocca, C. M.; Kaloyeros, A. E.; Williams, W. S. *J. Am. Chem. Soc.* **1987**, *109*, 1579−1580.
(8) Bhaviripudi, S.; Jia, X.; Dresselhaus, M. S.; Kong, J. *Nano Lett.* **2010**, *10*, 4128−4133.
(9) Li, X.; Cai, W.; Colombo, L.; Ruoff, R. S. *Nano Lett.* **2009**, *9*, 4268−4272.
(10) Page, A. J.; Minami, S.; Ohta, Y.; Irle, S.; Morokuma, K. *Carbon* **2010**, *48*, 3014−3026.
(11) Oznuluer, T.; Pince, E.; Polat, E. O.; Balci, O.; Salihoglu, O.; Kocabas, C. *Appl. Phys. Lett.* **2011**, *98*, 183101.
(12) *Handbook of Phase Diagrams of Metal Two Elements*; Chemical Industry Press: Qingnianhu Nanjie 13, Dongcheng District, Beijing, China; 2008.
(13) Klink, C.; Olesen, L.; Besenbacher, F.; Stensgaard, I.; Laegsgaard, E.; Lang, N. D. *Phys. Rev. Lett.* **1993**, *71*, 4350−4353.
(14) Nie, S.; Walter, A. L.; Bartelt, N. C.; Starodub, E.; Bostwick, A.; Rotenberg, E.; McCarty, K. F. *ACS Nano* **2011**, *5*, 2298−2306.
(15) Dong, G. C.; van Baarle, D. W.; Rost, M. J.; Frenken, J. W. M. *New J. Phys.* **2012**, *14*, 053033.
(16) Miniussi, E.; Pozzo, M.; Baraldi, A.; Vesselli, E.; Zhan, R. R.; Comelli, G.; Menteş, T. O.; Niño, M. A.; Locatelli, A.; Lizzit, S.; Alfè, D. *Phys. Rev. Lett.* **2011**, *106*, 216101.
(17) Tonnoir, C.; Kimouche, A.; Coraux, J.; Magaud, L.; Delsol, B.; Gilles, B.; Chapelier, C. *Phys. Rev. Lett.* **2013**, *111*, 246805.

(18) Papagno, M.; Moras, P.; Sheverdyaeva, P. M.; Doppler, J.; Garhofer, A.; Mittendorfer, F.; Redinger, J.; Carbone, C. *Phys. Rev. B: Condens. Matter Mater. Phys.* **2013**, *88*, 235430.
(19) Qi, Y.; Han, N.; Li, Y.; Zhang, Z.; Zhou, X.; Deng, B.; Li, Q.; Liu, M.; Zhao, J.; Liu, Z.; Zhang, Y. *ACS Nano* **2017**, *11*, 1807−1815.
(20) Gao, Y.; Zhang, Y.; Chen, P.; Li, Y.; Liu, M.; Gao, T.; Ma, D.; Chen, Y.; Cheng, Z.; Qiu, X.; Duan, W.; Liu, Z. *Nano Lett.* **2013**, *13*, 3439−3443.
(21) Liu, M.; Li, Y.; Chen, P.; Sun, J.; Ma, D.; Li, Q.; Gao, T.; Gao, Y.; Cheng, Z.; Qiu, X.; Fang, Y.; Zhang, Y.; Liu, Z. *Nano Lett.* **2014**, *14*, 6342−6347.
(22) Miniussi, E.; Pozzo, M.; Menteş, T. O.; Niño, M. A.; Locatelli, A.; Vesselli, E.; Comelli, G.; Lizzit, S.; Alfè, D.; Baraldi, A. *Carbon* **2014**, *73*, 389−402.
(23) Ramqvist, L. *J. Appl. Phys.* **1971**, *42*, 2113−2120.
(24) Chen, J. G. *Chem. Rev.* **1996**, *96*, 1477−1498.
(25) Stradi, D.; Barja, S.; Diaz, C.; Garnica, M.; Borca, B.; Hinarejos, J. J.; Sanchez-Portal, D.; Alcami, M.; Arnau, A.; de Parga, A. L. V.; Miranda, R.; Martin, F. *Phys. Rev. B: Condens. Matter Mater. Phys.* **2012**, *85*, 121404.
(26) Gall, N. R.; Mikhailov, S. N.; Rutkov, E. V.; Tontegode, A. Y. *Surf. Sci.* **1987**, *191*, 185−202.
(27) Sung, C.-M.; Tai, M.-F. *Int. J. Refract. Hard Met.* **1997**, *15*, 237−256.
(28) Domenichini, B.; Petigny, S.; Blondeau-Patissier, V.; Steinbrunn, A.; Bourgeois, S. *Surf. Sci.* **2000**, *468*, 192−202.
(29) Liu, M.; Gao, Y.; Zhang, Y.; Zhang, Y.; Ma, D.; Ji, Q.; Gao, T.; Chen, Y.; Liu, Z. *Small* **2013**, *9*, 1360−1366.
(30) Vinogradov, N. A.; Zakharov, A. A.; Kocevski, V.; Rusz, J.; Simonov, K. A.; Eriksson, O.; Mikkelsen, A.; Lundgren, E.; Vinogradov, A. S.; Martensson, N.; Preobrajenski, A. B. *Phys. Rev. Lett.* **2012**, *109*, 026101.
(31) Meschel, S. V.; Kleppa, O. J. *J. Alloys Compd.* **1997**, *257*, 227−233.
(32) Naguib, M.; Come, J.; Dyatkin, B.; Presser, V.; Taberna, P.-L.; Simon, P.; Barsoum, M. W.; Gogotsi, Y. *Electrochem. Commun.* **2012**, *16*, 61−64.
(33) Feibelman, P. J. *Surf. Sci.* **1981**, *103*, L149−L154.
(34) Feibelman, P. J. *Phys. Rev. B: Condens. Matter Mater. Phys.* **2008**, *77*, 165419.
(35) N'Diaye, A. T.; Bleikamp, S.; Feibelman, P. J.; Michely, T. *Phys. Rev. Lett.* **2006**, *97*, 215501.

DOI: 10.1021/jacs.7b09755
J. Am. Chem. Soc. 2017, 139, 17574−17581